Supplementary Information

Integrating Nitrogen Vacancies into Crystalline Graphitic Carbon Nitride for Enhanced Photocatalytic Hydrogen Production

Supplementary Information Includes:

EXPERIMENTAL SECTION

Text S1 Synthesis

Synthesis of CN: Pristine CN was prepared by the direct air-thermal polymerization of melamine. Typically, 5 g of melamine was placed into an alumina crucible with a cover. Then it was heated at 550 °C in the air for 4 hours with a heating rate of 10°C / min. The final products were collected after the temperature naturally was cooled down to the room temperature.

Synthesis of CN-NVs: 0.4 g of pristine CN was dispersed into the KOH aqueous solution (KOH: 0.1g, H_2O: 5 ml). The suspension was then ultrasonicated for 90 min and evaporated to dryness in an oven at 80 ^oC overnight. The obtained mixture was heated at 550 ^oC for 4 hours under the atmosphere of N_2. After it was naturally cooled down to the room temperature, the solid mixture was thoroughly washed with hot DI water several times to remove the alkali residual. The final products were dried overnight in an oven, denoted as CN-NVs.

Synthesis of CN-CTe: 0.4g of pristine CN was dispersed into the KCl/LiCl aqueous solution (KCl: 2.2 g, LiCl: 1.8 g, H_2O: 5 mL). The suspension was then ultrasonicated for 90 min and evaporated to dryness in an oven at 80 ^oC overnight. The obtained mixture was further heated at 550 ^oC for 4 hours under the atmosphere of N_2. After it was naturally cooled down to the room temperature, the solid mixture was thoroughly washed with hot DI water several times to remove the salt residual. The final products were dried overnight in an oven, denoted as CN-CTe.

Synthesis of CN-NVs-CTe: 0.4g of pristine CN was dispersed into the KCl/LiCl/KOH aqueous solution (KCl: 2.2g, LiCl: 1.8g, KOH: 0.1g, H_2O: 5 ml). The suspension was then ultrasonicated for 90 min and evaporated to dryness in an oven at 80 ^oC overnight. The obtained mixture was further heated at 550 ^oC for 4 hours under the atmosphere of N_2. After it was naturally cooled down to the room temperature, the solid mixture was thoroughly washed with hot DI water several times. The final products were dried overnight in an oven, denoted as CN-NVs-CTe.

Text S2 Characterization

Transmission electron microscope (TEM JEOL, JEM-2100F, Japan) was applied to

observe the morphologies of the samples. X-ray powder diffraction (XRD, D-MAX 2200 VPC, RIGAKU) was employed to obtain the crystal phase information. Attenuated total reflectance Fourier-transform infrared (ATR-FTIR, Nicolet IS10, Thermo Fisher Scientific, USA) spectroscopy and laser micro-Raman spectrometer (Renishaw inVia) were used to obtain the information of the different functional groups. X-ray photoelectron spectroscopy (XPS, ESCALAB 250Xi, Thermo, USA) was used to analyze the chemical composites. Electron Spin Resonance (ESR, Bruker A300) was carried out at 77K under dark condition to get the information of the nitrogen defects of materials. UV–Vis absorption spectroscopy (Shimadzu UV-2600) and photoluminescence spectroscopy (PL, Jobin Yvon Fluorolog-3-21) were conducted to investigate the optical properties of the samples. Time resolved fluorescence measurement (Horiba XH2612) was employed to detect the fluorescence lifetimes of the samples. Surface photo-voltage spectra (SPV, CEL-SPS1000, Beijing AuLight Co., Ltd) was used to get the information about the charge carrier separation and transformation. Surface photovoltage (SPV) measurements were recorded on a CEL-SPS1000 (Au-Light Co., Ltd) on the basis of the lock-in amplifier, including a lock-in amplifier (SR830, Stanford research systems, Inc.), monochromatic-light, a light chopper (SR540, Stanford research systems, Inc.), and a chamber. Monochromatic light was generated from a 150 W xenon lamp (CEL-S150) by a monochromator (CEL-IS151). Materials were used directly, and we constructed the photovoltaic cell as a sandwich-like architecture of FTO-sample-FTO. During the measurement, we aimed to standardize the samples by using the same sample mass on the same area of ITO.

Text S3 Photoelectrochemical experiments

Photoelectrochemical experiments were measured in a typical three-electrode cell system using an electrochemical workstation (Gamry Reference 3000, USA), where the as-prepared samples, Pt plate and Ag/AgCl electrode were used as working electrode, counter electrode and reference electrode, respectively. The working electrode was fabricated by using the following conventional procedure: 25 mg of sample was dispersed in 1 mL 0.005% nafion aqueous solution. Then, 0.2 mL of prepared suspension was spread on a piece of fluorine-doped tin oxide (FTO, 1.5 × 1.5 cm^2) glass slide. After natural dryness at room temperature, the FTO working electrode was further

dried at 353 K for 1 h to improve the adhesion. The photocurrent response was measured (light on/off mode) under 1.5G simulated solar light. Electrochemistry impedance spectroscopy (EIS) was performed under the frequency range of 5 mHz to 100 kHz with the 10 mV of amplitude current.

Text S4 Photocatalytic experiments

The photocatalytic hydrogen production experiments were performed in a commercial photoreactor (CEL-GSOA, Beijing AutLight Co., Ltd) which involves a 250 mL of Pyrex flask connected to a glass closed gas system and an autosampler connected with an online gas chromatograph (GC-2014C, SHIMADZU Co., Ltd) equipped with a thermal conductive detector (TCD). The reaction temperature was maintained at room temperature using a water-cooling system.

In a typical hydrogen production experiment, 25 mg of catalyst was dispersed into 100 mL of MeOH (10v/v %) aqueous solution. To verify the hydrogen production activities of CN, CN-NVs, CN-CTe and CN-NVs-CTe, an *in situ* photodeposition method using $PdCl_2$ solution was performed to load Pd (2 wt%) on the surface of the catalyst as a cocatalyst. After degassing treatment of the suspension, the sealed photoreactor was top-irradiated by a simulated sunlight (CEL-HXF300, Ceaulight Co. Ltd. Beijing, China). The evolved gases were automatically analyzed.

Text S5 Calculation methods

All the calculations were performed based on density functional theory (DFT) in this work, and the CASTEP modulus is implemented for geometry optimization, electron density difference and population analysis calculations. The exchange-correlation interactions were described by generalized gradient approximation (GGA) with the Perdew-Burke-Ernzerhof (PBE) functional.[1, 2] Spin-polarization was included in all calculations and a damped van der Waals correction was incorporated using Grimme's scheme to describe the non-bonding interactions.[3] All accuracy during calculating is set to Ultra-fine.

FIGURES & TABLES

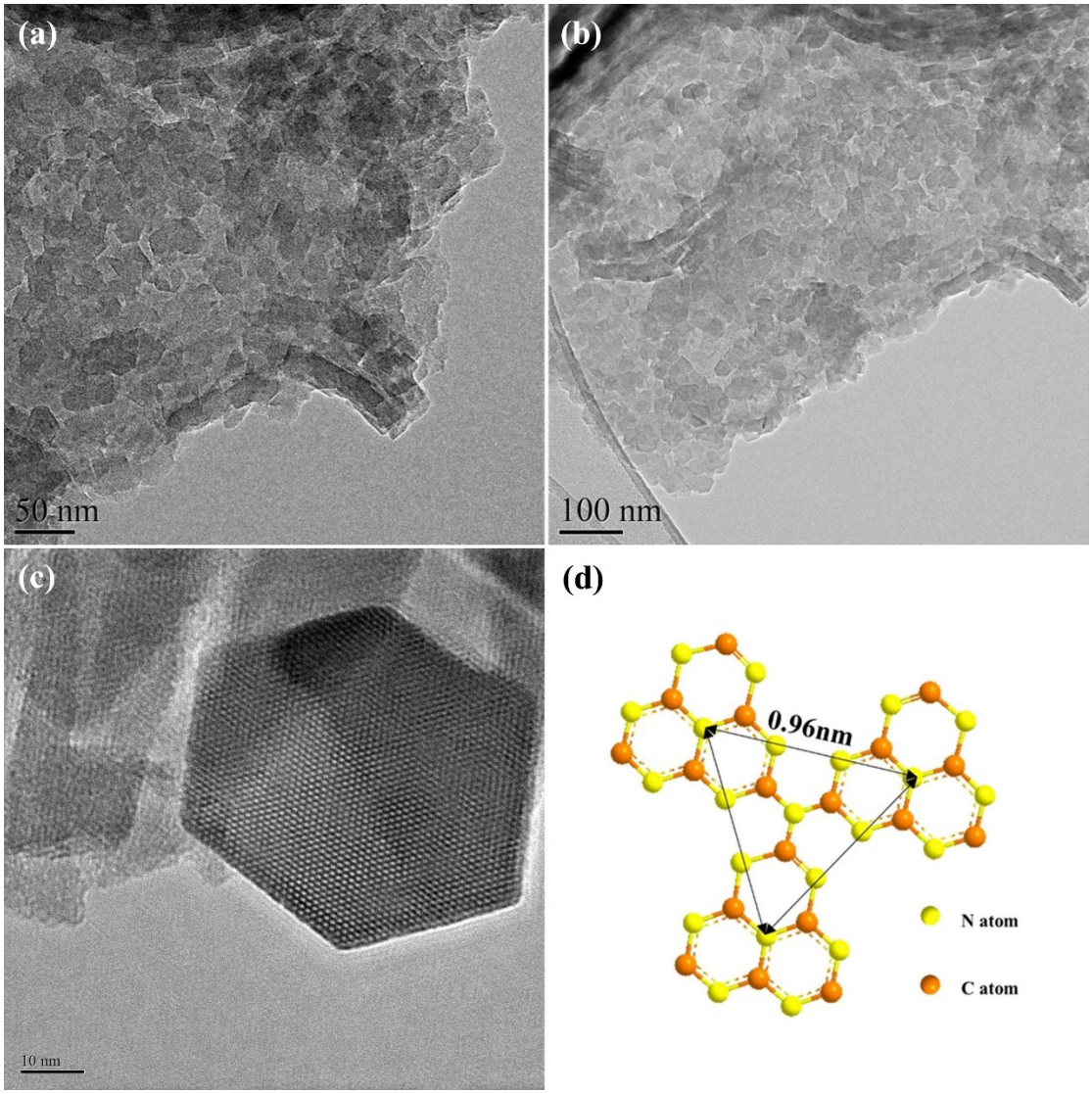

Figure S1 TEM images of CN-NVs-CTe (a-c) and structure model of CN-NVs-CTe unit

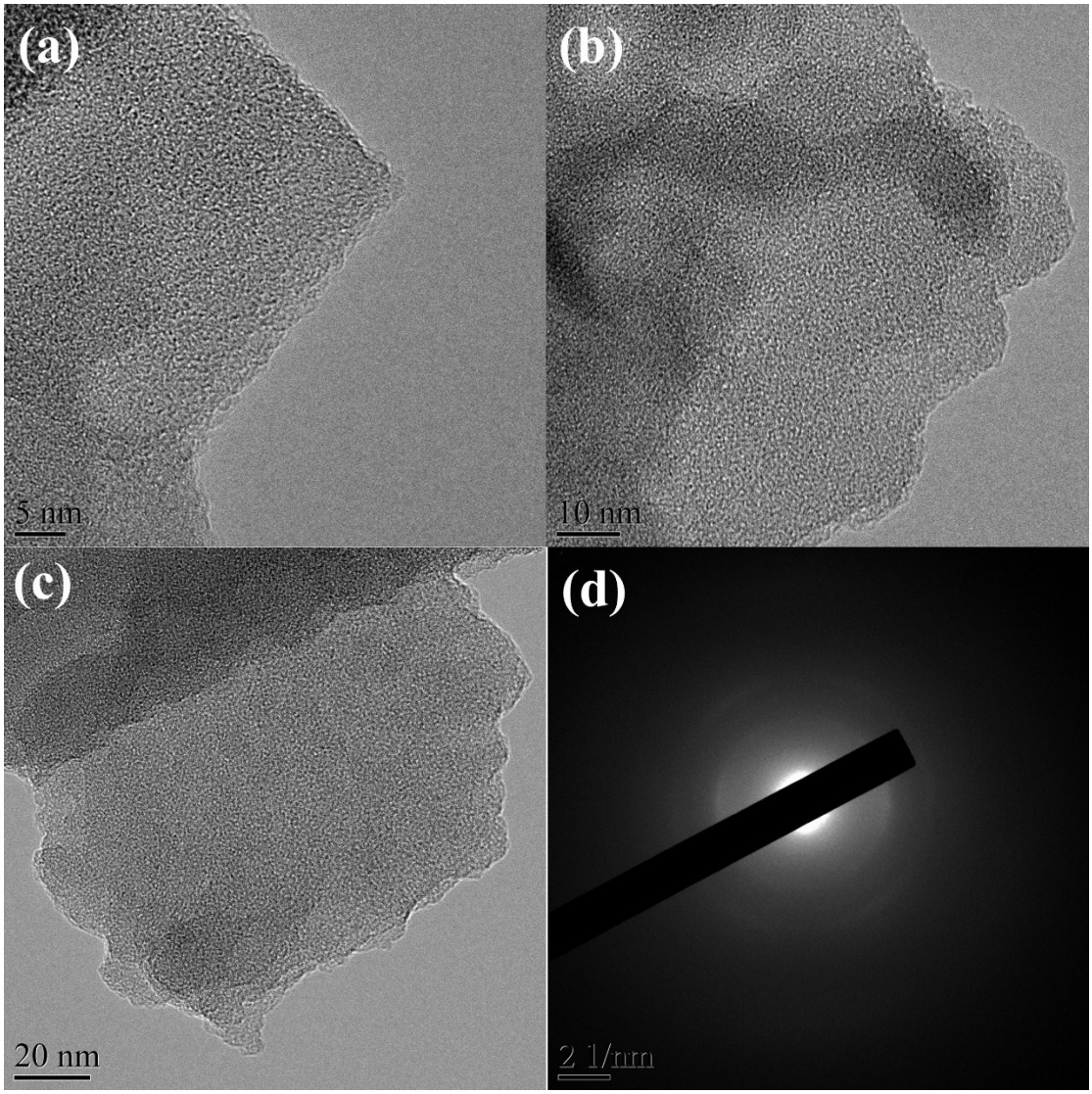

Figure S2 HRTEM images of pristine carbon nitride

Figure S2 shows that no crystal lattices were observed on the as-prepared pristine CN. Selected area electron diffraction (SAED) image confirms the amorphous structure of pristine CN.

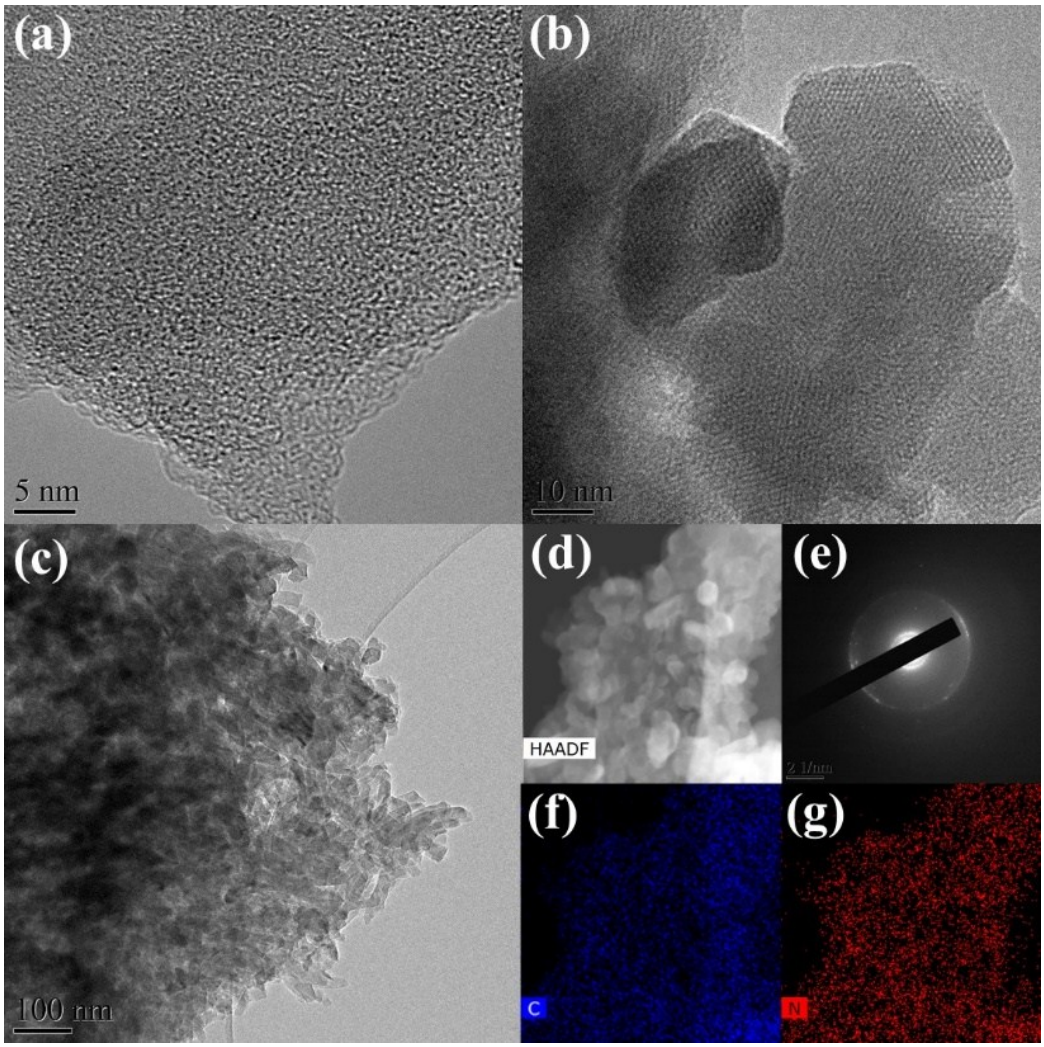

Figure S3 HRTEM images of (a) CN and (b-c) CN-CTe, (d) HAADF image, (e) selected area electron diffraction (SAED) and (f-g) EDX mapping images of CN-CTe.

Table S1 Elemental analysis of the different samples.

Sample	CN	CN-NVs	CN-CTe	CN-NVs-CTe
C/N ratio	0.6093	0.6478	0.6602	0.6796

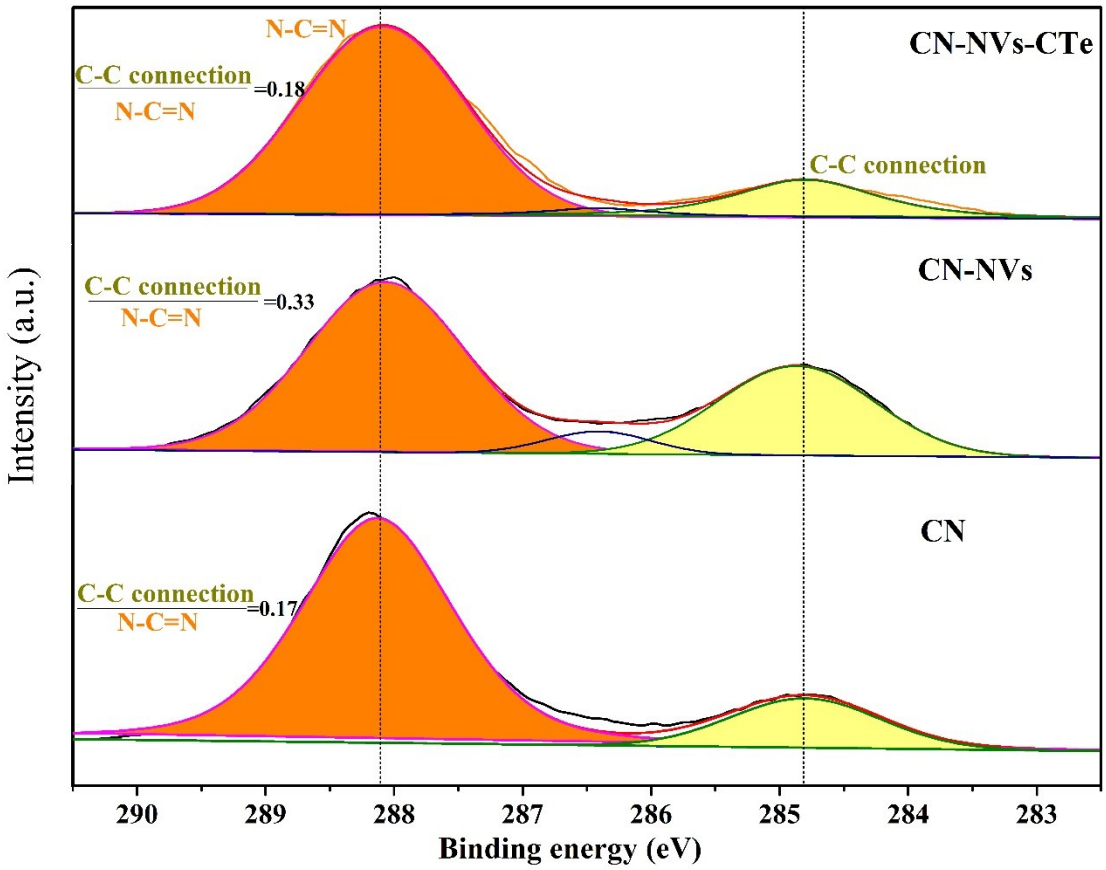

Figure S4 C1s XPS spectra of CN, CN-NVs and CN-NVs-CTe

Generally, the content of specified C atom (N-C=N and C-C in our case) was obtained through deconvoluting the C 1s XPS spectra and calculating the corresponding integral area. The (C- C)/(N-C=N) ratio is determined to be 0.17 in the bulk CN. For the CN-NVs, the ratio increases to 0.33, resulting from the generation of nitrogen vacancies. Interestingly, the ratio in CN-NVS-CTe is 0.18, which means that the enhanced rigidity inhibits the formation of C-C connection.

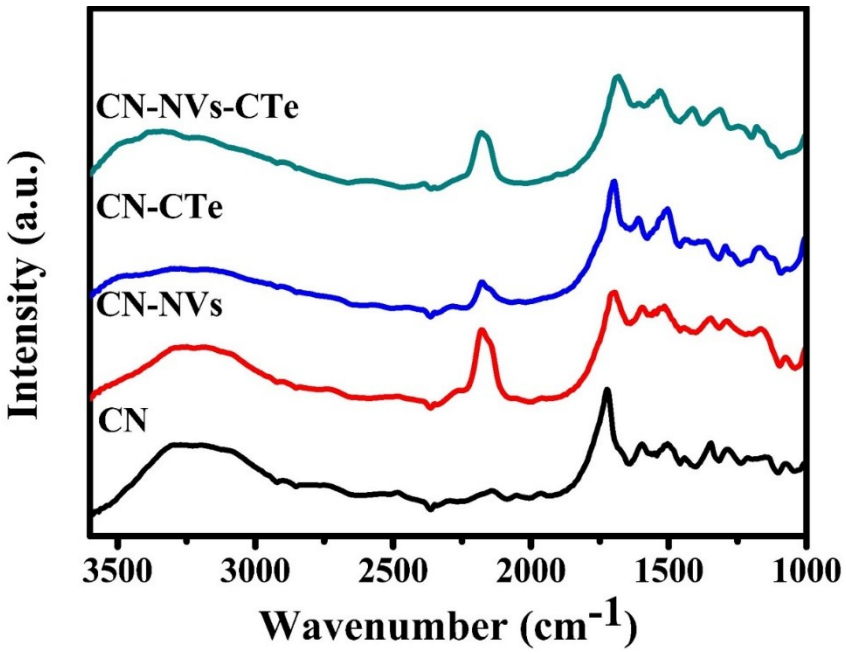

Figure S5 ATR-FTIR spectra of different samples

The surface structure of the as-prepared CNs was investigated using attenuated total reflection Fourier transform infrared spectroscopy (ATR-FTIR). As shown in Figure S4, multiple peaks between 900 and 1700 cm^{-1} correspond to the tri-s-triazine derivatives. All samples have the same peaks in this region, indicating that the molten salt method did not disrupt the basic CN units. The broad peak between 3000 and 3500 cm^{-1} is attributed predominantly to the stretching modes of the terminal amino groups, and the characteristic peak at 2150 cm^{-1} is attributed to an asymmetric stretching vibration of the cyano groups. With the use of KOH, the concentration of amino groups evidently decreases, and that of cyano groups increases remarkably, which suggests that the OH- reacts with the amine groups and attacks the CN moieties at high temperatures during the polymerization process, thus generating cyano groups.

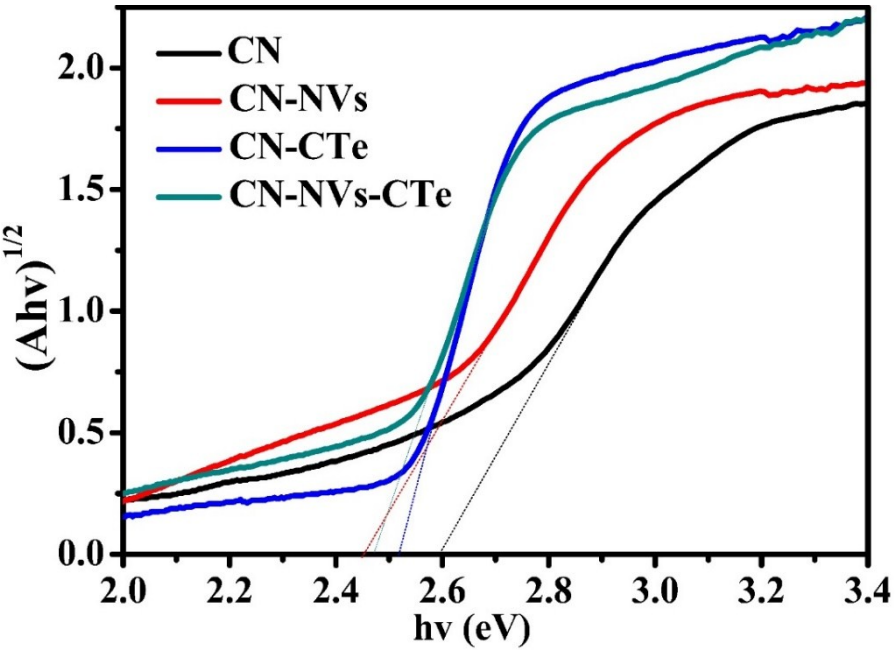

Figure S6 Plots of transformed kubelka-Munk function versus photon energy for different samples

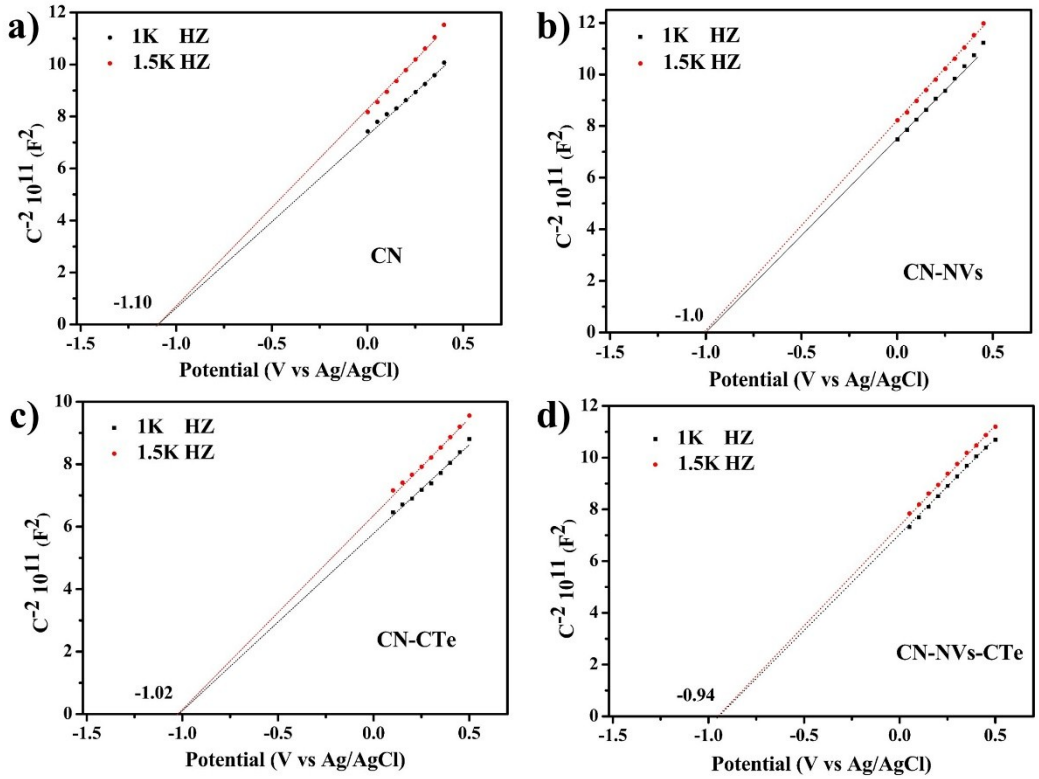

Figure S7 Mott-Schottky plot of a) CN, b) CN-NVs, c) CN-CTe, and d) CN-NVs-CTe

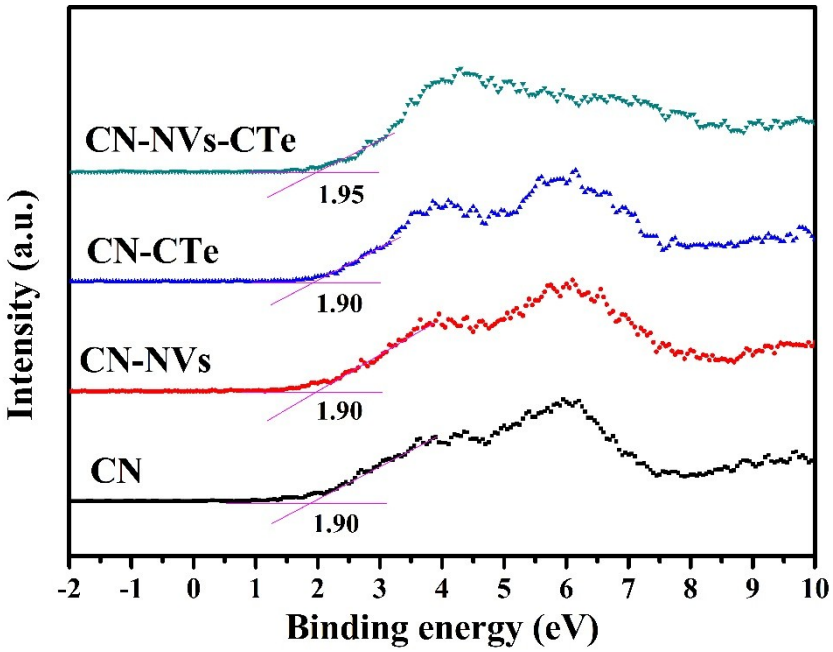

Figure S8 VBXPS spectra of as-prepared samples

The VB maximum was similar for CN, CN-NVs, CN-CTe, CN-NVs-CTe (1.90, 1.90, 1.90 and 1.95eV). The contact potential difference between the samples and the analyzer was estimated to be ≈1.68, 1.68, 1.68 and 1.73eV versus normal hydrogen electrode (NHE) at pH 7 using the formula (a). (Yu et al., Adv. Mater. 2017, 1605148). And the corresponding VB were also calculated using the formula (b) and (c) though MS plot and DRS spectra. The following is summarized result which indicates these band position measured by Mott-Schottky plot is in good agreement with the result calculated from the DRS and VB-XPS.

$$E_{VB/NHE} = \Phi + E_{VBXPS} - 4.44 \quad \text{(a)}$$

$$E_{CB/NHE} = E_{MS/Ag/AgCl} + 0.2046V \quad \text{(b)}$$

$$E_{VB} = E_{CB} + E_{band\ gap} \quad \text{(c)}$$

NHE: potential of normal hydrogen electrode; Φ of 4.22 eV: the electron work function of the analyzer. E_{VBXPS} ： The potential measured by VBXPS; $E_{MS/Ag/AgCl}$: The potential measured by Mott-Schottky plots using Ag/AgCl as a reference electrode in 0.1M $NaSO_4$; 0.2046 v: The value is the normal hydrogen electrode of Ag/AgCl electrode in

0.1M $NaSO_4$.

Table S2 VB potential obtain from VBXPS and MS plot

VB potential	CN	CN-NVs	CN-CTe	CN-NVs-CTe
$E_{NHE/VBXPS}$ (V)	1.68	1.68	1.68	1.73
$E_{NHE/MS}$(V)	1.70	1.65	1.70	1.73

Table S3. Kinetic parameters of the fitting decay parameters of different samples.

Sample	A1	τ1	A2	τ2	A3	τ3	$\tau_{Average}$ (ns)
CN	2284.31	2.08034	2880.883	2.08039	99.77076	9.52274	2.684948611
CN-NVs	18.44944	16.80193	3244.17	1.80153	3204.943	1.80136	2.191289202
CN-CTe	31.22491	13.76289	3417.992	1.70874	4297.528	1.7085	2.089157751
CN-NVs-CTe	2320.583	1.67491	2349.499	1.67503	2279.377	1.67512	1.675019453

Fitting equation:

$$y=A_1\times exp(\frac{-x}{\tau_1})+A_2\times exp(\frac{-x}{\tau_2})+A_3\times exp(\frac{-x}{\tau_3})$$

Average lifetime equation:

$$\tau_{average}=\frac{A_1\times\tau_1^2+A_2\times\tau_2^2+A_3\times\tau_3^2}{A_1\times\tau_1+A_2\times\tau_2+A_3\times\tau_3}$$

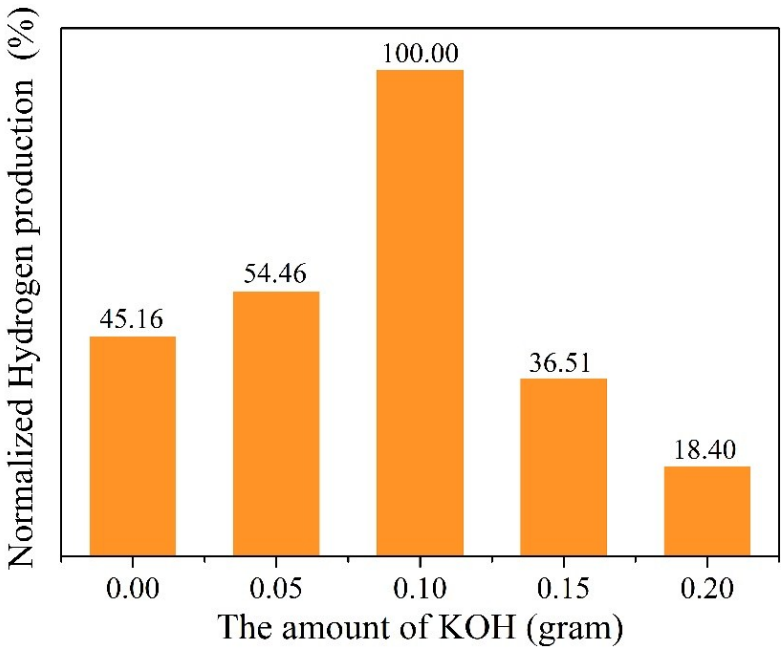

Figure S9 Effect of KOH amount during the synthetic process on the photocatalytic activity

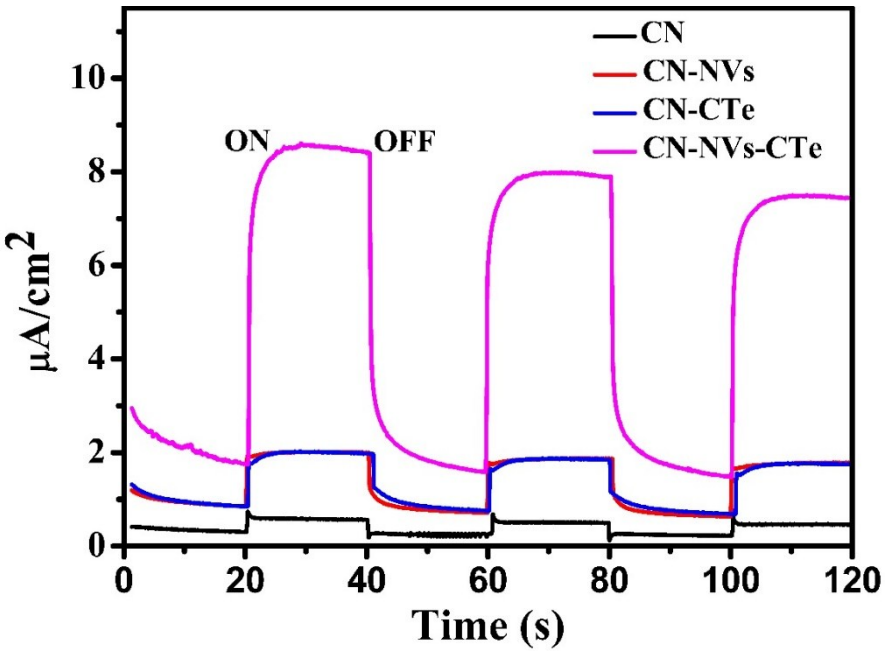

Figure S10 Transient photocurrent of the prepared samples

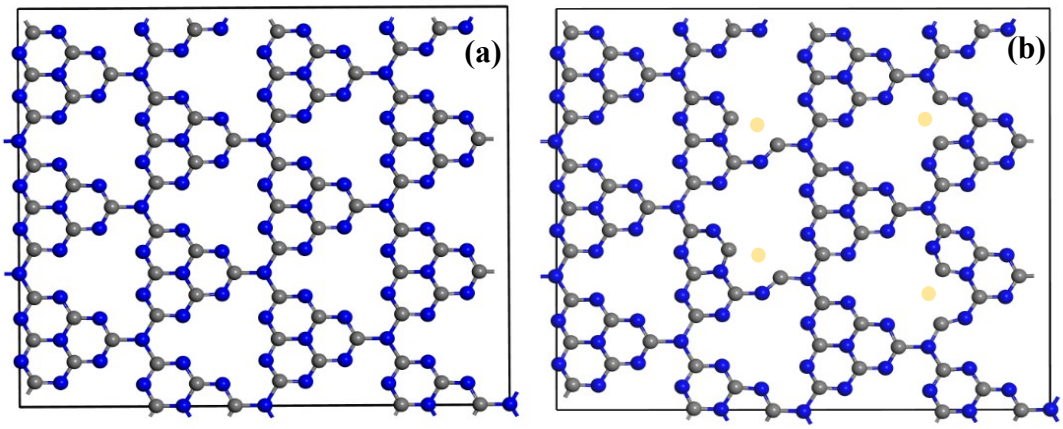

Figure S11 The optimized structures of CN-CTe (a) and CN-NVs-CTe (b). The nitrogen vacancies are marked by yellow circles.

Figure S11a presents the optimized structure for CN-CTe, which contains one single atomic layer. The supercell used in our simulation is 3*2*1 with a vacuum width of 12 Å. The vacuum space is considered to be big enough to eliminate the interaction between the layers in supercells. All atoms are allowed to relax in all energy calculations. In order to investigate the effects of nitrogen vacancies, the supercell of CN-NVs-CTe is built, as shown in Figure S12b.

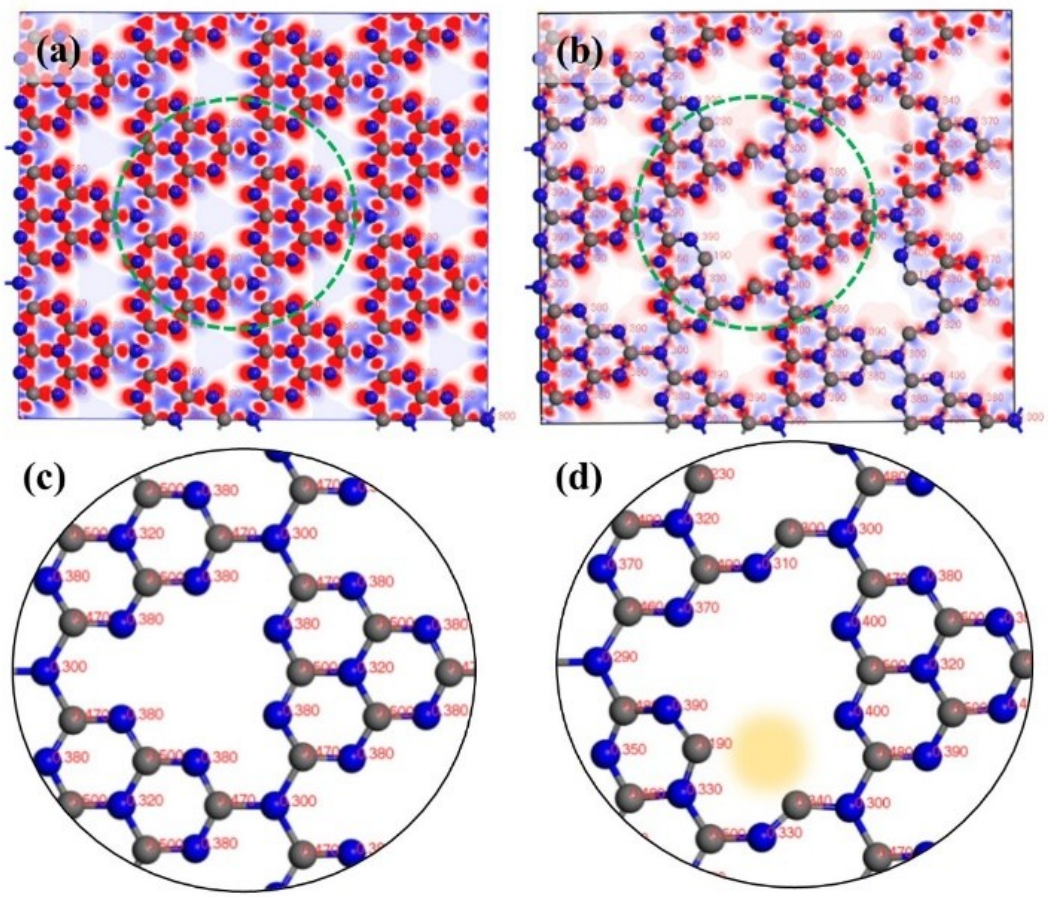

Figure S12 Electron density and population analysis of CN-CTe (a) and CN-NVs-CTe (b). (c) and (d) are the detailed population charges of the green dotted circle in figure (a) and (b).

References

1. T. Liao, C. Sun, A. Du, Z. Sun, D. Hulicova-Jurcakova and S. Smith, *Journal of Materials Chemistry*, 2012, **22**, 8321-8326.
2. J. P. Perdew, K. Burke and M. Ernzerhof, *Physical Review Letters*, 1996, **77**, 3865-3868.
3. A. Du, S. Sanvito, Z. Li, D. Wang, Y. Jiao, T. Liao, Q. Sun, Y. H. Ng, Z. Zhu, R. Amal and S. C. Smith, *Journal of the American Chemical Society*, 2012, **134**, 4393-4397.